Title
Phenylalanine Monitoring via Aptamer-Field-Effect Transistor Sensors

Journal
ACS Sensors, 4(12)

ISSN
2379-3694

Authors
Cheung, Kevin M
Yang, Kyung-Ae
Nakatsuka, Nako
et al.

Publication Date
2019-12-27

DOI
10.1021/acssensors.9b01963

Peer reviewed

HHS Public Access

Author manuscript

ACS Sens. Author manuscript; available in PMC 2020 January 13.

Published in final edited form as:

ACS Sens. 2019 December 27; 4(12): 3308–3317. doi:10.1021/acssensors.9b01963.

Phenylalanine Monitoring *via* Aptamer-Field-Effect Transistor Sensors

Kevin M. Cheung[1,2], **Kyung-Ae Yang**[3], **Nako Nakatsuka**[1,2], **Chuanzhen Zhao**[1,2], **Mao Ye**[1,2], **Michael E. Jung**[1,2], **Hongyan Yang**[4], **Paul S. Weiss**[1,2,5,*], **Milan N. Stojanović**[3,6,*], **Anne M Andrews**[1,2,4,*]

[1]Department of Chemistry and Biochemistry, University of California, Los Angeles, Los Angeles, California 90095, United States

[2]California NanoSystems Institute, University of California, Los Angeles, Los Angeles, California 90095, United States

[3]Department of Medicine, Columbia University, New York, New York 10032, United States

[4]Department of Psychiatry and Biobehavioral Sciences, Semel Institute for Neuroscience & Human Behavior, and Hatos Center for Neuropharmacology, University of California, Los Angeles, Los Angeles, California 90095, United States

[5]Departments of Bioengineering and Materials Science and Engineering, University of California, Los Angeles, Los Angeles, California 90095, United States

[6]Departments of Biomedical Engineering and Systems Biology, Columbia University, New York, New York 10032, United States

Abstract

Determination of the amino acid phenylalanine is important for lifelong disease management in patients with phenylketonuria, a genetic disorder in which phenylalanine accumulates and persists at levels that alter brain development and cause permanent neurological damage and cognitive dysfunction. Recent approaches for treating phenylketonuria focus on injectable medications that efficiently break down phenylalanine but sometimes result in detrimentally low phenylalanine levels. We have identified new DNA aptamers for phenylalanine in two formats, initially as fluorescent sensors and then, incorporated with field-effect transistors (FETs). Aptamer-FET sensors detected phenylalanine over a wide range of concentrations (fM-mM). *para*-

*To whom correspondence should be addressed: aandrews@mednet.ucla.edu, mns18@cumc.columbia.edu, psw@cnsi.ucla.edu.

Author Contributions

All authors designed the experiments. KMC, KAY, NN, CZ, and HY carried out the experiments. MY and MEJ were responsible for the PEPA synthesis. All authors performed data analysis and interpreted the results. KMC, KAY, NN, PSW, MNS, and AMA wrote the manuscript with input from all authors.

Supporting Information

The Supporting Information is available free of charge on the ACS Publications website at doi: 10.1021/acssensors.9b01963. Additional methods and characterization of phenylalanine and phenylalanine rhodium-complex aptamers, phenylalanine aptamer control experiments, FET transfer curves, circular dichroism spectra, HPLC analysis of mouse serum samples, NMR spectrum of PEPA, optical microscopy images, and phenylalanine aptamer sequences.

NN, KAY, PSW, MNS, and AMA have an international patent on stem-loop receptor-based field-effect devices for sensing in physiological salt concentrations, International application PCT/US2019/046891. MNS has patent applications, a start-up company, and consulting income for work on small-molecule aptamers.

Chlorophenylalanine, which inhibits the enzyme that converts phenylalanine to tyrosine, was used to induce hyperphenylalaninemia during brain development in mice. Aptamer-FET sensors were specific for phenylalanine *vs para*-chlorophenylalanine and differentiated changes in mouse serum phenylalanine at levels expected in patients. Aptamer-FETs can be used to investigate models of hyperphenylalanemia in the presence of structurally related enzyme inhibitors, as well as naturally occurring amino acids. Nucleic acid-based receptors that discriminate phenylalanine analogs, some that differ by a single substituent, indicate a refined ability to identify aptamers with binding pockets tailored for high affinity and specificity. Aptamers of this type integrated into field-effect transistors enable rapid, electronic, label-free phenylalanine sensing.

Graphical Abstract

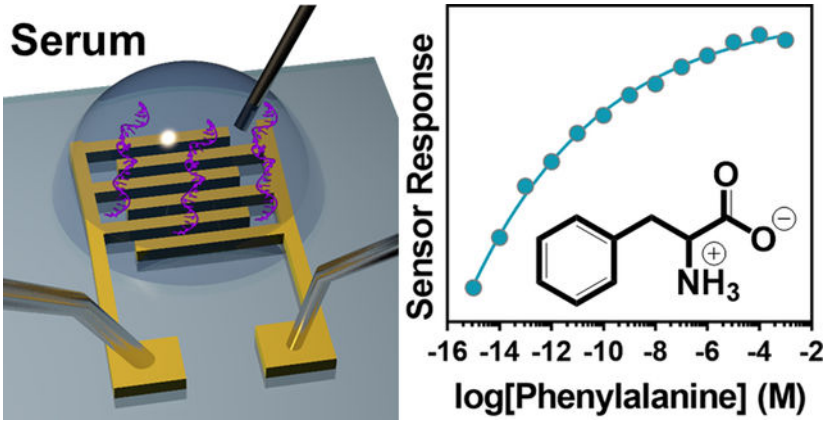

Keywords

Phenylketonuria; DNA; electronic sensor; serum; amino acid

INTRODUCTION

Phenylketonuria (PKU) is an autosomal recessive genetic disorder involving mutations in the gene that encodes phenylalanine hydroxylase (PAH), a liver enzyme that converts the essential amino acid phenylalanine to tyrosine (Figure 1A).[1–7] In the United States, PKU occurs in ~1/10,000–15,000 babies yearly. Diagnosis at birth is critical.[1,3,4,7,8] This ‘inborn error of metabolism’ leads to hyperphenylalaninemia in the blood and brain.[1–5,7,9] Elevated phenylalanine causes abnormalities in brain development associated with permanent intellectual impairment. Screening newborns for PKU involves laboratory testing by a bacterial inhibition assay, *i.e.*, the Guthrie test,[10] or more recently, tandem mass spectrometry.[11] Although sufficient for diagnosis, these methods involve turnaround times of days to inform treatment providers and families.[12]

Phenylketonuria is primarily managed through strict avoidance of phenylalanine-containing foods.[1,3,4,7,13,14] Early-life dietary management largely prevents the damaging effects of PKU on brain development.[15–17] However, even modestly uncontrolled blood phenylalanine levels in children and adults have been correlated with cognitive and psychiatric sequelae.

[1,7,18–21] Nevertheless, studies on this topic are sparse, partly because technologies for straightforward monitoring of blood phenylalanine levels in clinical studies are not readily available.[1,18]

Phenylalanine serum concentrations in healthy individuals are 60±30 μM.[17] Current treatment guidelines for individuals with PKU are to maintain blood phenylalanine levels between 120 and 360 μM. Moderate hyperphenylalaninemia is associated with blood levels ranging from 360 to 600 μM, while untreated PKU is characterized by phenylalanine levels >1000 μM (with concentrations >3000 μM having been reported).[1,3,7,22]

Emerging treatments for PKU are based on enzyme replacement with pegylated versions of bacterial phenylalanine ammonia lyase.[23] Enzyme substitution decreases phenylalanine levels in patients with PKU and reduces the need for dietary restrictions, which can be exceedingly difficult to maintain over a lifetime.[23] In 2017, the U.S. Food and Drug Administration approved the first enzyme substitution therapy, pegvaliase (Palynziq™).[23] However, pegvaliase and related treatment strategies can result in hypophenylalaninemia, which negatively affects protein synthesis, and thus, growth in children, and neurotransmitter synthesis in children and adults.[17,23] In light of the present clinical picture, improvements in phenylalanine monitoring are indicated to provide insights into the pharmacokinetics[24] and efficacy of current and future PKU treatment strategies and their combinations.[25] Enabling patients to determine their own blood phenylalanine levels will be empowering. Regardless, there are no at-home or point-of-care options for measuring phenylalanine.[26–28]

Field-effect transistors (FETs) modified with protein receptors have been developed for rapid electronic, reagentless detection of biological targets.[29–37] Receptor recognition of charged targets and/or target-induced receptor reorientation gate the semiconductor channels of FETs to modulate transconductance. However, bioFETs based on protein receptors or antibodies are not feasible for direct sensing in biological fluids because large receptors (~10 nm) are too far away from semiconductor channels relative to the Debye screening length. At physiological ion concentrations, the Debye length is on the order of 1 nm.[30,38]

Recently, we developed thin-film metal oxide FETs functionalized with oligonucleotide stem-loop receptors (aptamers).[39–42] We discovered that target-mediated reorganization of a portion of the highly negatively charged backbones of small oligonucleotides (and rearrangement of associated counter ions) occurs near enough to the semiconductor surfaces to circumvent Debye-length limitations under biological conditions.[43–46] Aptamer-FETs have enabled sensitive and selective detection of small molecules, including neutral targets, in physiological buffers and fluids, and complex biological matrices.[30]

Here, previously unreported aptamers for direct phenylalanine detection were coupled with nanometer-thin In_2O_3 FETs. Phenylalanine was detected over many orders of magnitude in physiological solutions. Selectivity for phenylalanine over closely structured endogenous and exogenous aromatic amino acid analogs (Figure 1B) and metabolites was excellent, particularly for one of the phenylalanine aptamers. Phenylalanine sensing was carried out in serum from mice with induced hyperphenylalaninemia, demonstrating the ability of

aptamer-FETs to detect biologically important differences in phenylalanine concentrations. Aptamer sequences were rationally modified to shift device sensitivities towards physiologically relevant concentrations. These findings portend the use of aptamer-functionalized FETs for phenylalanine monitoring in PKU patients and other relevant populations.

Experimental Section

No unexpected or unusually high safety hazards were encountered.

Materials

All materials were purchased from Sigma-Aldrich Co. (St. Louis, MO), unless otherwise noted. The amino acids used throughout were the L-forms, *i.e.*, L-phenylalanine (Sigma P5482 and P2126), L-tyrosine (Sigma T3754), and L-tryptophan (Sigma 93659 and T0254). Oligonucleotides were obtained from Integrated DNA Technologies (Coralville, IA). The SYLGARD 184 used to make polydimethylsiloxane (PDMS) wells was from Dow Corning Corporation (Midland, MI). Water was deionized before use (18.2 MΩ) with a Milli-Q system (Millipore, Billerica, MA).

para-Ethynylphenylalanine (PEPA) was synthesized by a previously reported route[47] with minor modifications. Trimethylsilyl acetylene was coupled under palladium catalysis to to *N*-acetyl 4-iodophenylalanine methyl ester,[48] followed by deprotection and purification. The nuclear magnetic resonance spectroscopy (NMR) data matched spectra reported in the literature (Figure S1).

Phenylalanine aptamer selection

Phenylalanine aptamer selection was carried out as per a previously reported strategy.[41] Initial selection resulted in isolation of an aptamer for phenylalanine complexed with pentamethylcyclopentadienyl rhodium(III) (Cp*Rh). This previously reported aptamer, which we designate Phe-Cp*Rh 1, showed cross-reactivity with the analogous tryptophan-Cp*Rh complex (Trp-Cp*Rh), limiting its use in practical applications. To reduce cross-reactivity, additional selections for Phe-Cp*Rh were performed with Trp-Cp*Rh counter-selection,[41,42] which resulted in the isolation of two new Phe-Cp*Rh aptamers, which we designate Phe-Cp*Rh 2 and Phe-Cp*Rh 3 (Table S1). These previously unreported Phe-Cp*Rh aptamers were not cross-reactive with Trp-Cp*Rh (Figure S2C,S3). However, Phe-Cp*Rh 2 showed cross reactivity with Tyr-Cp*Rh (Figure S2C).

Unexpectedly, as byproducts of the selections for additional Phe-Cp*Rh aptamers, we identified three aptamers that directly recognize phenylalanine, rather than the Phe-Cp*Rh complex. These previously unreported, direct-binding aptamers are designated Phe 1, Phe 2, and Phe 3 (Table S1). An excess of phenylalanine (1 mM) was used in the selection procedures to produce the Phe-Cp*Rh complex such that Cp*Rh was the limiting reagent. Under these conditions, a large excess of free phenylalanine, which also interacted with the oligonucleotide sequences, was present along with the Phe-Cp*Rh complex in the target solutions. We compared the responses of Phe 1 to phenylalanine with and without Cp*Rh

(Figure S4). In the presence of Cp*Rh, phenylalanine prefers to complex with Cp*Rh, however the remaining free phenylalanine in solution was detected by Phe 1.

Fluorescence assays were carried out in 20 mM HEPES, 1 M NaCl, 10 mM $MgCl_2$, and 5 mM KCl (pH 7.5) using a Victor II microplate reader (PerkinElmer). Each aptamer sequence was modified with fluorescein at the 5' end. Complementary strands were 3'-modified with dabcyl for solution quenching determination of dissociation constants (K_d) (Table S1) and for selectivity testing. Concentrations of aptamers and complementary strands were empirically determined and aptamer K_d values were calculated as per previously published methods.[30,40,41] Putative aptamer secondary structures shown were predicted using *Mfold* (http://unafold.rna.albany.edu/?q=mfold).

Aptamer-functionalized field-effect transistors

Field-effect transistors were fabricated using ~4 nm In_2O_3 semiconductor films as channel materials with high surface-to-volume ratios. Aqueous solutions (0.1 M) of indium(III) nitrate hydrate ($In(NO_3)_3 \cdot xH_2O$, 99.999%) were spin-coated at 3000 rpm for 30 s onto heavily doped silicon wafers (University Wafer, Boston, MA or WaferPro, San Jose, CA) with 100-nm thermally grown oxide layers. After coating, substrates were pre-heated at 150 °C for 10 min followed by 3 h of annealing at 350 °C.[29,49] Source and drain electrodes (10 nm Ti/30 nm Au) were deposited by electron-beam evaporation and patterned *via* standard photolithography.

To functionalize thin-film FETs with thiolated phenylalanine aptamers, we first self-assembled mixed monolayers of (3-aminopropyl)trimethoxysilane and trimethoxy(propyl)silane (1:9 v/v ratio) using vapor-phase deposition on In_2O_3 surfaces at 40 °C for 1 h. Substrates were then incubated with a 1 mM ethanolic solution of 1-dodecanethiol for 1 h to passivate Au electrodes *via* alkanethiol monolayer formation. After rinsing with ethanol, substrates were incubated with a 1 mM solution of 3-maleimidobenzoic acid *N*-hydroxysuccinimide ester (MBS) in 1:9 (v/v) dimethyl sulfoxide and phosphate-buffered saline (1× PBS, pH 7.4) for 30 min. Thiolated DNA aptamers (Table S2) were diluted to 1 μM in nuclease-free water and heated for 5 min at 95 °C followed by rapid cooling in an ice bath. Substrates were then immersed in aptamer solutions for 24 h, rinsed with deionized water, and dried under N_2 gas.

A scrambled aptamer sequence for Phe 3 was designed using *mfold* to have a secondary structure that was predicted to differ from the correct phenylalanine aptamer sequence, while maintaining the same numbers and types of nucleotides (Figure S5B and Table S2).

Field-effect transistor measurements

Polydimethylsiloxane wells were sealed on individual FETs to hold sensing solutions. Substrates had inter-FET distances (~2 mm) that were large enough to enable isolation of single FET devices within the PDMS wells (Figure S6). Ringer's solution (147 mM NaCl, 4 mM KCl, 2.25 mM $CaCl_2$) was used as the electrolyte solution. The Ag/AgCl reference electrodes (World Precision Instruments, Inc., Sarasota, FL) were placed in sensing solutions in a top-gate (solution-gate) device configuration. Measurements were performed using a

manual analytical probe station (Signatone, Gilroy, CA) equipped with a Keithley 4200A-SCS (Tektronix, Beaverton, OR) semiconductor parameter analyzer.

Source-drain current (I_{DS}) transfer curves were obtained wherein gate voltages (V_{GS}) were varied from 0 to 400 mV with a step voltage of 5 mV. The drain voltage (V_D) was held at 10 mV throughout. Five sweeps were averaged for each transfer curve. Calibrated responses were calculated by dividing the absolute sensor response (ΔI), which takes into account baseline subtraction, by the change in source-drain current with voltage sweep ($\Delta I_{DS}/\Delta V_G$).[50] Aptamer-FET responses at V_G=375 mV were used to calculate mean calibrated responses.

Mouse serum

Mice were generated at the University of California, Los Angeles (UCLA) from a core colony of a serotonin transporter (SERT)-deficient lineage maintained on a mixed CD1 × 129S6/SvEv background *via* heterozygous SERT-deficient (SERT+/−) pairings. For this study, three pairs of SERT wildtype (SERT+/+) mice from the core colony were bred to produce 18 wildtype pups. All mice were maintained on a 12-h light/dark cycle (lights on at 0600 h (Zeitgeber time 0)) with *ad libitum* food and water. The Association for Assessment and Accreditation of Laboratory Animal Care International has fully accredited UCLA. All animal care and use met the requirements of the NIH Guide for the Care and Use of Laboratory Animals, revised 2011. The UCLA Chancellor's Animal Research Committee (Institutional Animal Care and Use Committee) preapproved all procedures.

For postnatal treatment, pups from each litter were randomly assigned to one of three groups: (1) Saline (vehicle control); (2) 100 mg/kg *para*-chlorophenylalanine (Sigma #C3635);[51] or (3) 10 mg/kg *para*-ethynylphenylalanine.[52] Doses were calculated based on the free base form of each compound. The pH values of PEPA and PCPA saline were adjusted to pH 7.4 prior to injection. Dosing solutions were filtered *via* 0.22 μm filters for sterilization.

Each litter contained all treatment groups. Each pup received a subcutaneous injection of the assigned treatment daily during ZT 6–8 on postnatal days (P)4–21. The injection volume was 10 mL/kg during P4–11, and 5 mL/kg during P12–21. A total of three of the 18 pups were excluded from this study: 1/6 saline-treated and 1/6 PCPA-treated subjects died during the postnatal period. In addition, 1/6 PEPA-treated subjects stopped receiving injections at P17 due to body weight loss for two continuous days. The data from the remaining N=5 mice per treatment group are reported.

Pups were weaned after the last injection on P21 and housed with their same-sex siblings. Two hours after the last injection, subjects were euthanized by decapitation under deep anesthesia with isoflurane. Whole blood samples were collected *via* cardiac puncture and placed in microcentrifuge tubes pre-chilled on ice for 30–60 min. Following coagulation, blood samples were centrifuged at 16,000 g for 15 min at 4 °C twice. After each centrifugation, supernatants were removed and transferred to clean microcentrifuge tubes on ice.

Serum samples were aliquoted and stored at −80 °C until analysis. Aptamer-FET and high performance liquid chromatography (HPLC) measurements were carried out by investigators blind to the treatment group identification of each sample. All serum samples for aptamer-FET measurements were diluted to ~10 pM phenylalanine in 1× Ringer's buffer, using the same serial dilution strategy, *i.e.*, first 1:10, then 1:100, and finally 1:1.5, which was based on the average phenylalanine concentration determined in mouse serum by HPLC.

Circular dichroism spectroscopy

Intensities and positions of positive and negative peaks for oligonucleotides in circular dichroism (CD) spectra correspond to exciton interactions induced by stacking of hydrophobic bases in asymmetric helices.[45,46,53] Aptamer and target concentrations were 2 μM in 1× Ringer's buffer. Thiolated aptamers were heated at 95 °C for 5 min and cooled to room temperature slowly to relax DNA molecules into extended conformations. Spectra were collected using a JASCO J-715 circular dichroism spectrophotometer (Oklahoma City, OK). Four scans with 0.5-nm resolution, 1.0-nm bandwidth, a 4-s response time, and a 20 nm/min scan rate were acquired per sample. Scans of 1× Ringers solution were subtracted as background.

Statistics

Data for fluorescence assays and FET calibrated responses are reported as means ± standard errors of the means and were analyzed using GraphPad Prism 7.04 (GraphPad Software Inc., San Diego, CA) *via* one-way analysis of variance followed by Tukey's multiple comparisons *post hoc* tests. Cross-validation data for phenylalanine levels were analyzed by linear regression analysis. In all cases, $P<0.05$ was considered statistically significant.

RESULTS AND DISCUSSION

Three previously unreported DNA aptamer sequences that directly recognize the amino acid phenylalanine were identified *via* solution-phase, *in vitro* systematic evolution of ligands by exponential enrichment (SELEX) (Figure 1C–E).[39,41,42] Dissociation constants were determined using competitive fluorescence assays.[30,40,41] Quencher-labeled complementary sequences (Table S1 and Figure S7) were displaced from fluorescently labeled aptamer sequences upon phenylalanine binding resulting in increases in fluorescence intensities, as shown in Figure 1C–E.[30,40,41] Solution dissociation constants (K_d) were 10 μM, 7 μM, and 16 μM for Phe 1, Phe 2, and Phe 3, respectively. Dissociation constants measured for Phe 1 and 2 *via* dye displacement assays were consistent with those measured *via* competitive binding assays (Figure S8). Dye displacement did not work for the Phe 3 aptamer. This result is sometimes the case for dye displacement, which is why we do not use this method as a primary means of determining dissociation constants.

Selections initially had been carried out using a strategy to try to increase aptamer selectivity towards low epitope targets by associating targets with metal complexes.[41] In addition to a previously reported aptamer sequence recognizing phenylalanine complexed with pentamethylcyclopentadienyl rhodium(III) (Cp*Rh) (sequence herein referred to as Phe-

Cp*Rh 1),[41] two previously unreported sequences, Phe-Cp*Rh 2 and Phe-Cp*Rh 3 were characterized (Figures S2,S3).

Selectivity testing for the three direct-detection phenylalanine aptamers using competitive florescence assays showed reduced (Phe 1 and Phe 2) or negligible (Phe 3) responses towards the endogenous aromatic amino acids tyrosine and tryptophan (Figure 1C–E). We also investigated selectivity of the direct-detection phenylalanine aptamers for two phenylalanine analogs, *para*-chlorophenylalanine (PCPA) and *para*-ethynylphenylalanine (PEPA) (Figure 1B), which potentially induce hyperphenylalaninemia in animal models (*vide infra*).[54–58] The Phe 3 aptamer showed minimal responses to PCPA or PEPA *via* competitive fluorescence assays (Figure 1E), in contrast to Phe 1 and Phe 2 (Figure 1C–D), and the Phe-Cp*Rh aptamers (Figure S9), all of which had appreciable responses to PCPA.

Next, each of the phenylalanine-specific aptamers was attached to the semiconducting channels of FETs for electronic detection of phenylalanine (Figure 2A).[29,30] As in our prior aptamer-FET studies, shortened,[59,60] thiolated aptamers were attached to In_2O_3 surfaces *via* covalent modification to self-assembled silanes using *m*-maleimidobenzoyl-*N*-hydroxysuccinimide as a crosslinker.[29,30] Field-effect transistors were operated in a top-gate setup. The source-drain current (I_{DS}) was measured while sweeping the gate voltage (V_{GS}) during target exposure (Figure 2A).[29,30] Reorganization of surface-tethered negatively charged oligonucleotides occurred in close proximity to metal-oxide semiconducting surfaces upon target capture to gate FET transconductances resulting in target-concentration-dependent current changes under physiological ionic conditions (Figure 2B).[30]

Phenylalanine-aptamer-FETs showed a wide range of concentration-dependent responses to phenylalanine (fM detection limit) in 1× Ringer's solution, which mimics the ionic composition of the plasma fraction of human blood (Figure 2B). Sensing in physiological buffers that have similar ion concentrations to the target biological matrix is important for evaluating oligonucleotide receptors because interactions with different types and concentrations of solution ions may result in alternate aptamer secondary structures and thus, differences in sensor sensitivities and selectivities.[61,62]

We also tested one of the aptamers recognizing phenylalanine complexed with Cp*Rh when attached to FETs, as an example of the use of this type of aptamer. The Phe-Cp*Rh 2 aptamer showed similar concentration-dependent responses (Figure S2D) to those of the direct detection sequences (Figure 2B), suggesting that metal complexation to increase sensitivity, which would complicate point-of-care or at-home monitoring approaches, is unnecessary[41] and direct phenylalanine detection is sufficient in the context of FET sensors.

Target-concentration-dependent decreases in current were observed for FET transfer curves (I_{DS}-V_{GS} sweeps) for each of the three direct sensing aptamers (Figures 2C,S10). We attribute decreases in FET transfer characteristics on *n*-type semiconductors to a dominant effect of negatively charged DNA aptamer backbones moving closer to semiconductor channel surfaces to increase electrostatic repulsion of charge carriers (band bending) and to gate transconductance upon target binding.[30] We previously determined that aptamer-FET small-molecule sensing is due to gating associated with the reorganization of charged DNA

aptamer backbones and not to target charge. Target-aptamer interaction can reorient aptamer charge toward or away from semiconductor channels, based on specific aptamers.[30]

We performed circular dichroism (CD) spectroscopy to investigate target-induced changes in aptamer secondary structures for the three phenylalanine direct-sensing aptamers, as we have been able to associate CD spectral changes with individual aptamer-FET responses.[30] The spectra for Phe 3 showed a small but reproducible decrease in peak intensity at 280 nm after target capture, potentially corresponding to target-induced formation of hairpin motifs (Figure 2D).[53] Spectra showed negligible changes in peak positions or intensities for Phe 1 or Phe 2 upon association with phenylalanine (Figure S11). These findings suggest that the latter two aptamers do not form new secondary structural motifs upon target recognition and that all three aptamers primarily undergo adaptive target binding largely involving pre-formed secondary structures.[30]

Of the three direct-detection phenylalanine aptamers, Phe 3 showed the largest target-related responses and the smallest replication variability when integrated with FETs (Figure 2B). The Phe 3 aptamer also showed the highest selectivity towards nonspecific targets compared to Phe 1 and Phe 2 in competitive fluorescence assays (Figure 1C–E); thus, we focused on investigating this sequence further. To test selectivity on FETs, we measured the responses of Phe 3-aptamer-FETs to the aromatic amino acid tryptophan, the phenylalanine metabolites tyrosine, phenylpyruvic acid, and 2-phenylethylamine, and the two phenylalanine analogs (Figure 2E). Sensor responses upon exposure to 100 μM solutions of five of the nonspecific targets were <10% of the average response to an equivalent concentration of phenylalanine; responses to PCPA were 15% of the average phenylalanine response. Concentrations of nonspecific targets were selected based on their physiologically relevant concentrations.[63–65] As a further indication of selectivity, responses of FETs functionalized with a scrambled version of the Phe 3 sequence having the same numbers and types of nucleotides as the correct Phe 3 aptamer sequence but with a different predicted secondary structure were negligible (Figure S5).

To investigate Phe 3-aptamer-FET detection of clinically relevant phenylalanine levels, we measured phenylalanine in serum (diluted with 1× Ringers, see Experimental Section) from mice injected daily with PCPA, PEPA, or saline during postnatal days 4–21 (Figure 3A). This postnatal period in mice is the human developmental equivalent of the last trimester of pregnancy and the first postnatal year.[66,67] We selected this treatment period because it is important for determining the impact of elevated phenylalanine levels on cortical axon development.[68] Both *para*-substituted phenylalanine analogs inhibit tryptophan hydroxylase (TPH), which converts dietary tryptophan to 5-hydroxytryptophan. The latter is decarboxylated to produce the neurotransmitter serotonin (5-hydroxytryptamine).[52,69–71] However, whereas PCPA has been reported to inhibit PAH activity, in addition to TPH,[54–58] PEPA has been suggested to lack inhibitory effects on PAH.[52]

Mice receiving PCPA showed a doubling of the concentration of serum phenylalanine levels (individual levels ranging from ~90 to 160 μM) compared to mice exposed to PEPA or saline (Figure 3B). Phenylalanine concentrations in mouse serum samples were cross-validated *via* HPLC with electrochemical detection (Figure S12 and Supplemental Methods). Individual

phenylalanine serum sample levels determined using aptamer-FETs were highly correlated when compared to those measured by HPLC (R^2=0.95; Figure 3C). The slope of the regression line correlating phenylalanine levels determined by both methods was ~1 indicating that Phe 3-aptamer-FETs accurately reported phenylalanine levels.

Phenylalanine levels detected by aptamer-FETs in PCPA-treated mice (~120 μM) were at the low end of the range of serum levels in humans with modestly elevated phenylalanine, *i.e.*, PKU patients adhering to dietary restrictions, and possibly, phenylalanine levels in some PKU carriers, *i.e.*, individuals with one mutant PAH allele (*ca.* one in 50 Caucasians)[72,73]. Thus, aptamer-FETs can be used to differentiate modest yet physiologically relevant changes in phenylalanine levels.

The Phe 3 aptamer-FETs were sufficient to detect biologically relevant differences in phenylalanine levels in diluted serum (Figure 3). Removing base pairs from aptamer stem regions destabilizes aptamer secondary structures, particularly in stem-loop aptamers isolated by solution SELEX where stem closure plays an important role in identifying target-specific sequences.[59,74–76] We reasoned that stem truncation could be used to shift aptamer-FET sensitivity ranges closer to the therapeutic range of PKU patients, thereby reducing the need for serum dilution.

Strategically deleting complementary C-G base pairs (C-G base pairs form three hydrogen bonds *vs.* A-T base pairs, which are weaker in forming only two H-bonds) in the stem regions of Phe 1 and Phe 3 (Table S2) shifted the corresponding aptamer-FET concentration curves to the right, *i.e.*, towards higher phenylalanine concentrations (Figure 4). These modifications also increased the steepness of the concentration curves such that small differences in phenylalanine levels in the steepest regions of these curves would be more highly differentiable.

Notably, the serum phenylalanine concentration range in PKU patients is ~10–1000 μM.[1] Thus, narrowing the sensitivity range of aptamer-FET sensors, in addition to reducing the binding affinity, *i.e.*, shifting to higher K_d, advances this strategy toward an at-home monitoring scenario wherein phenylalanine might be determined in whole blood from finger or heel sticks without the need for dilution. Stem destabilization, in addition to decreasing aptamer densities,[30] and/or tuning FET characteristics[77] and measurement parameters can eventually be combined to achieve phenylalanine detection in undiluted blood.

There are numerous benefits and opportunities for at-home phenylalanine monitoring. In a National Institutes of Health (NIH) consensus panel on “PKU: screening and management”, the NIH recommended the development of reliable home testing methods for measuring phenylalanine to increase adherence to dietary treatments.[78] There is consensus from PKU patients that at-home measurement of phenylalanine will make disease management, *i.e.*, following a PKU diet and/or enzyme substitution dosing, easier to achieve and to maintain throughout life.[26] National Institutes of Health guidelines for monitoring frequency in PKU patients are once weekly during the first year of life, twice per month for individuals 1–12 years of age, and at least monthly thereafter. In women with PKU prior to and during pregnancy and lactation, frequency should increase to at least weekly.

Phenylalanine has been determined using chromatographic,[79,80] plasmonic,[81] and fluorimetric techniques.[79,82–84] These methods involve specialized laboratory instrumentation and sometimes, complex extractions. As such, these methods are largely incompatible with point-of-care or at-home monitoring. Colorimetric, paper-based detection platforms show promise for PKU diagnosis and monitoring in low-resource settings,[85,86] but use enzyme-based recognition elements, which can lose activity over time due to denaturation.[87] Electrochemical signal transduction has been used for phenylalanine sensing[88,89] or a conductive electrode design involving graphene oxide, which is intrinsically defect prone and synthetically heterogeneous.[90] Hasanzadeh and coworkers[91,92] reported an electrochemical strategy involving phenylalanine capture *via* a previously reported RNA phenylalanine aptamer (K_d~120 μM)[93] followed by phenylalanine oxidation at gold electrodes. Compared to RNA, aptamers comprised of DNA are advantageous in terms of higher stability when exposed to biological matrices, such as serum.[94]

CONCLUSIONS AND PROSPECTS

We have identified three new DNA-based receptors that recognize the biochemically and medically important target phenylalanine. We also report two new aptamers that recognize a phenylalanine-organometallic complex (Phe-Cp*Rh). The direct-binding phenylalanine aptamers (and one of the Phe-Cp*Rh aptamers) were integrated with thin-film metal-oxide field-effect transistors (FETs). Phenylalanine-FET sensors detected phenylalanine under physiological ionic conditions over six orders of magnitude with fM detection limits. Sensors incorporating the Phe 3 direct-detection aptamer showed exceptional selectivity for phenylalanine *vs.* similarly structured aromatic amino acids and metabolites. The accuracy and precision of Phe 3 aptamer-FET sensors were excellent compared to a gold-standard laboratory method.[62]

The ability to differentiate clinically relevant differences in serum phenylalanine levels with a minimal dilution step demonstrates the capability of aptamer-FETs for future use in electronic point-of-care devices for PKU diagnosis and management. In principle, aptamer-FET sensors can also be used for *in vivo* monitoring to investigate transiently induced or permanently maintained (through continuous administration of PCPA or *via* mice with constitutive reductions in PAH)[95] elevations in phenylalanine. Rapid monitoring in PKU animal models will enable investigating how changes in PAH activity or diet impact temporally resolved phenylalanine levels.

In sum, DNA aptamers are readily synthesized[96] and the FET fabrication methods used here are straightforward and easily scaled up. We have miniaturized[29] and nanostructured[77] In_2O_3 thin-film FETs using low-cost soft-lithographic methods.[97–99] We have also fabricated In_2O_3 FETs on flexible substrates[100] demonstrating capabilities to tailor device performance and architectures for specific biomedical applications.

Aptamer-FET sensors can be rapidly deployed, with minor adjustments, at the point-of-care level, *e.g.*, in clinical laboratories. While not the focus of this work, we have developed prototype instrumentation and analysis software that is low-cost, has a relatively small footprint, and can perform multiplexed FET sensing. Translation for at-home monitoring

will require additional development of FET-measurement technology to reduce size for portability, *i.e.*, hand-held devices, and validation in clinical samples.[101] We anticipate that phenylalanine sensing *via* aptamer-FETs will improve phenylketonuria disease management and monitoring in other at-risk populations.

Supplementary Material

Refer to Web version on PubMed Central for supplementary material.

ACKNOWLEDGMENTS

This research was supported by funding from the National Institute on Drug Abuse (DA045550) and Aptatek Biosciences. The authors thank Xinyi Cheng, Angela Leeway, and Victoria Wang for assistance with mouse serum collection, Dr. John M. Abendroth for assistance with circular dichroism interpretation, Dr. Olena Lukoyanova for assistance with NMR spectroscopy, and Dr. Mirelis Cancel-Santos for feedback on the manuscript. Figure 3A was created with Biorender.com. The authors acknowledge the use of instruments at the UCLA-DOE Biochemistry Instrumentation Core Facility and the UCLA Molecular Instrumentation Center.

REFERENCES

(1). Blau N; van Spronsen FJ; Levy HL Phenylketonuria. Lancet 2010, 376, 1417–1427. [PubMed: 20971365]

(2). Friedman PA; Kaufman S; Song Kang E Nature of the Molecular Defect in Phenylketonuria and Hyperphenylalaninaemia. Nature 1972, 240, 157–159. [PubMed: 4118080]

(3). Mitchell JJ; Trakadis YJ; Scriver CR Phenylalanine Hydroxylase Deficiency. Genet. Med 2011, 13, 697–707. [PubMed: 21555948]

(4). Scriver CR; Clow CL Phenylketonuria: Epitome of Human Biochemical Genetics. N. Engl. J. Med 1980, 303, 1336–1342. [PubMed: 7001231]

(5). Scriver CR The *PAH* Gene, Phenylketonuria, and a Paradigm Shift. Hum. Mutat 2007, 28, 831–845. [PubMed: 17443661]

(6). Penrose L; Quastel JH Metabolic Studies in Phenylketonuria. Biochem. J 1937, 31, 266–274. [PubMed: 16746333]

(7). Vockley J; Andersson HC; Antshel KM; Braverman NE; Burton BK; Frazier DM; Mitchell J; Smith WE; Thompson BH; Berry SA Phenylalanine Hydroxylase Deficiency: Diagnosis and Management Guideline. Genet. Med 2013, 16, 188–200. [PubMed: 24385074]

(8). Guttler F Hyperphenylalaninemia: Diagnosis and Classification of the Various Types of Phenylalanine Hydroxylase Deficiency in Childhood. Acta Paediatr. Scand 1980, 280, 1–80.

(9). Fölling A Über Ausscheidung von Phenylbrenztraubensäure in den Harn als Stoffwechselanomalie in Verbindung mit Imbezillität. Hoppe-Seyler's Z. Physiol. Chem 1934, 227, 169–176.

(10). Guthrie R Blood Screening for Phenylketonuria. JAMA 1961, 178, 863–863.

(11). Chace DH; Millington DS; Terada N; Kahler SG; Roe CR; Hofman LF Rapid Diagnosis of Phenylketonuria by Quantitative Analysis for Phenylalanine and Tyrosine in Neonatal Blood Spots by Tandem Mass Spectrometry. Clin. Chem 1993, 39, 66–71. [PubMed: 8419060]

(12). Seashore MR; Wappner R; Cho S; de la Cruz F; Wappner R; Cho S; Kronmal RA; Schuett V; Seashore MR Management of Phenylketonuria for Optimal Outcome: A Review of Guidelines for Phenylketonuria Management and a Report of Surveys of Parents, Patients, and Clinic Directors. Pediatrics 1999, 104, e68. [PubMed: 10586002]

(13). Bickel H; Gerrard J; Hickmans EM The Influence of Phenylalanine Intake on the Chemistry and Behaviour of a Phenylketonuria Child. Acta Paediatr. 1954, 43, 64–77. [PubMed: 13138177]

(14). Armstrong MD; Tyler FH Studies on Phenylketonuria I. Restricted Phenylalanine Intake in Phenylketonuria. J. Clin. Invest 1955, 34, 565–580. [PubMed: 14367510]

(15). Walter JH; White FJ; Hall SK; MacDonald A; Rylance G; Boneh A; Francis DE; Shortland GJ; Schmidt M; Vail A How Practical are Recommendations for Dietary Control in Phenylketonuria? Lancet 2002, 360, 55–57. [PubMed: 12114043]

(16). Waisbren SE; Mahon BE; Schnell RR; Levy HL Predictors of Intelligence Quotient and Intelligence Quotient Change in Persons Treated for Phenylketonuria Early in Life. Pediatrics 1987, 79, 351–355. [PubMed: 3822635]

(17). Longo N; Dimmock D; Levy H; Viau K; Bausell H; Bilder DA; Burton B; Gross C; Northrup H; Rohr F; Sacharow S; Sanchez-Valle A; Stuy M; Thomas J; Vockley J; Zori R; Harding CO Evidence- and Consensus-Based Recommendations for the Use of Pegvaliase in Adults with Phenylketonuria. Genet. Med 2018, DOI: 10.1038/s41436-41018-40403-z.

(18). Cleary M; Trefz F; Muntau AC; Feillet F; van Spronsen FJ; Burlina A; Bélanger-Quintana A; Giżewska M; Gasteyger C; Bettiol E; Blau N; MacDonald A Fluctuations in Phenylalanine Concentrations in Phenylketonuria: A Review of Possible Relationships with Outcomes. Mol. Genet. Metab 2013, 110, 418–423. [PubMed: 24090706]

(19). Arnold GL; Kramer BM; Kirby RS; Plumeau PB; Blakely EM; Cregan LSS; Davidson PW Factors Affecting Cognitive, Motor, Behavioral and Executive Functioning in Children with Phenylketonuria. Acta Paediatr. 2007, 87, 565–570.

(20). Anastasoaie V; Kurzius L; Forbes P; Waisbren S Stability of Blood Phenylalanine Levels and IQ in Children with Phenylketonuria. Mol. Genet. Metab 2008, 95, 17–20. [PubMed: 18703366]

(21). Hood A; Grange DK; Christ SE; Steiner R; White DA Variability in Phenylalanine Control Predicts IQ and Executive Abilities in Children with Phenylketonuria. Mol. Genet. Metab 2014, 111, 445–451. [PubMed: 24568837]

(22). Viau KS; Wengreen HJ; Ernst SL; Cantor NL; Furtado LV; Longo N Correlation of Age-Specific Phenylalanine Levels with Intellectual Outcome in Patients with Phenylketonuria. J. Inherited Metab. Dis 2011, 34, 963–971. [PubMed: 21556836]

(23). Markham A Pegvaliase: First Global Approval. Biodrugs 2018, 32, 391–395. [PubMed: 30022433]

(24). Arroyo-Currás N; Ortega G; Copp DA; Ploense KL; Plaxco ZA; Kippin TE; Hespanha JP; Plaxco KW High-Precision Control of Plasma Drug Levels Using Feedback-Controlled Dosing. ACS Pharmacol. Transl. Sci 2018, 1, 110–118.

(25). Cross R How Phenylketonuria, a Once-Neglected Disease, Became a Proving Ground for New Drugs Chem. Eng. News, 7 2019, pp 24.

(26). Bilginsoy C; Waitzman N; Leonard CO; Ernst SL Living with Phenylketonuria: Perspectives of Patients and Their Families. J. Inherited Metab. Dis 2005, 28, 639–649. [PubMed: 16151894]

(27). Wendel U; Langenbeck U Towards Self-Monitoring and Self-Treatment in Phenylketonuria — A Way to Better Diet Compliance. Eur. J. Pediatr 1996, 155, S105–S107. [PubMed: 8828623]

(28). Clarke SF; Foster JR A History of Blood Glucose Meters and Their Role in Self-Monitoring of Diabetes Mellitus. Br. J. Biomed. Sci 2012, 69, 83–93. [PubMed: 22872934]

(29). Kim J; Rim YS; Chen H; Cao HH; Nakatsuka N; Hinton HL; Zhao C; Andrews AM; Yang Y; Weiss PS Fabrication of High-Performance Ultrathin In_2O_3 Film Field-Effect Transistors and Biosensors Using Chemical Lift-Off Lithography. ACS Nano 2015, 9, 4572–4582. [PubMed: 25798751]

(30). Nakatsuka N; Yang K-A; Abendroth JM; Cheung KM; Xu X; Yang H; Zhao C; Zhu B; Rim YS; Yang Y; Weiss PS; Stojanović MN; Andrews AM Aptamer–Field-Effect Transistors Overcome Debye Length Limitations for Small-Molecule Sensing. Science 2018, 362, 319–324. [PubMed: 30190311]

(31). Schöning MJ; Poghossian A Recent Advances in Biologically Sensitive Field-Effect Transistors (BioFETs). Analyst 2002, 127, 1137–1151. [PubMed: 12375833]

(32). Allen BL; Kichambare PD; Star A Carbon Nanotube Field-Effect-Transistor-Based Biosensors. Adv. Mater 2007, 19, 1439–1451.

(33). Curreli M; Zhang R; Ishikawa FN; Chang H; Cote RJ; Zhou C; Thompson ME Real-Time, Label-Free Detection of Biological Entities Using Nanowire-Based FETs. IEEE Trans. Nanotechnol 2008, 7, 651–667.

(34). Li B-R; Hsieh Y-J; Chen Y-X; Chung Y-T; Pan C-Y; Chen Y-T An Ultrasensitive Nanowire-Transistor Biosensor for Detecting Dopamine Release from Living PC12 Cells Under Hypoxic Stimulation. J. Am. Chem. Soc 2013, 135, 16034–16037. [PubMed: 24125072]

(35). So H-M; Won K; Kim YH; Kim B-K; Ryu BH; Na PS; Kim H; Lee J-O Single-Walled Carbon Nanotube Biosensors Using Aptamers as Molecular Recognition Elements. J. Am. Chem. Soc 2005, 127, 11906–11907. [PubMed: 16117506]

(36). Green NS; Norton ML Interactions of DNA with Graphene and Sensing Applications of Graphene Field-Effect Transistor Devices: A Review. Anal. Chim. Acta 2015, 853, 127–142. [PubMed: 25467454]

(37). Lung Khung Y; Narducci D Synergizing Nucleic Acid Aptamers with 1-Dimensional Nanostructures as Label-Free Field-Effect Transistor Biosensors. Biosens. Bioelectron 2013, 50, 278–293. [PubMed: 23872609]

(38). Vacic A; Criscione JM; Rajan NK; Stern E; Fahmy TM; Reed MA Determination of Molecular Configuration by Debye Length Modulation. J. Am. Chem. Soc 2011, 133, 13886–13889. [PubMed: 21815673]

(39). Nutiu R; Li Y *In Vitro* Selection of Structure-Switching Signaling Aptamers. Angew. Chem. Int. Ed 2005, 44, 1061–1065.

(40). Yang K-A; Pei R; Stefanovic D; Stojanović MN Optimizing Cross-Reactivity with Evolutionary Search for Sensors. J. Am. Chem. Soc 2012, 134, 1642–1647. [PubMed: 22142383]

(41). Yang K-A; Barbu M; Halim M; Pallavi P; Kim B; Kolpashchikov DM; Pecic S; Taylor S; Worgall TS; Stojanović MN Recognition and Sensing of Low-Epitope Targets via Ternary Complexes with Oligonucleotides and Synthetic Receptors. Nat. Chem 2014, 6, 1003–1008. [PubMed: 25343606]

(42). Yang K-A; Pei R; Stojanović MN In Vitro Selection and Amplification Protocols for Isolation of Aptameric Sensors for Small Molecules. Methods 2016, 106, 58–65. [PubMed: 27155227]

(43). Xiao Y; Uzawa T; White RJ; DeMartini D; Plaxco KW On the Signaling of Electrochemical Aptamer-Based Sensors: Collision- and Folding-Based Mechanisms. Electroanalysis 2009, 21, 1267–1271. [PubMed: 20436787]

(44). Neumann O; Zhang D; Tam F; Lal S; Wittung-Stafshede P; Halas NJ Direct Optical Detection of Aptamer Conformational Changes Induced by Target Molecules. Anal. Chem 2009, 81, 10002–10006. [PubMed: 19928834]

(45). Liu W; Fu Y; Zheng B; Cheng S; Li W; Lau T-C; Liang H Kinetics and Mechanism of Conformational Changes in a G-Quadruplex of Thrombin-Binding Aptamer Induced by Pb^{2+}. J. Phys. Chem. B 2011, 115, 13051–13056. [PubMed: 21950308]

(46). Nagatoishi S; Tanaka Y; Tsumoto K Circular Dichroism Spectra Demonstrate Formation of the Thrombin-Binding DNA Aptamer G-Quadruplex Under Stabilizing-Cation-Deficient Conditions. Biochem. Biophys. Res. Commun 2007, 352, 812–817. [PubMed: 17150180]

(47). Kayser B; Altman J; Beck W Alkyne Bridged α- Amino Acids by Palladium Mediated Coupling of Alkynes with N-t-boc-4-Iodo-Phenylalanine Methyl Ester. Tetrahedron 1997, 53, 2475–2484.

(48). Lowary T; Meldal M; Helmboldt A; Vasella A; Bock K Novel Type of Rigid C-Linked Glycosylacetylene–Phenylalanine Building Blocks for Combinatorial Synthesis of C-Linked Glycopeptides. J. Org. Chem 1998, 63, 9657–9668.

(49). Chen H; Rim YS; Wang IC; Li C; Zhu B; Sun M; Goorsky MS; He X; Yang Y Quasi-Two-Dimensional Metal Oxide Semiconductors Based Ultrasensitive Potentiometric Biosensors. ACS Nano 2017, 11, 4710–4718. [PubMed: 28430412]

(50). Ishikawa FN; Curreli M; Chang H-K; Chen P-C; Zhang R; Cote RJ; Thompson ME; Zhou C A Calibration Method for Nanowire Biosensors to Suppress Device-to-Device Variation. ACS Nano 2009, 3, 3969–3976. [PubMed: 19921812]

(51). Alexandre C; Popa D; Fabre V; Bouali S; Venault P; Lesch K-P; Hamon M; Adrien J Early Life Blockade of 5-Hydroxytryptamine 1A Receptors Normalizes Sleep and Depression-Like Behavior in Adult Knock-Out Mice Lacking the Serotonin Transporter. J. Neurosci 2006, 26, 5554–5564. [PubMed: 16707806]

(52). Stokes AH; Xu Y; Daunais JA; Tamir H; Gershon MD; Butkerait P; Kayser B; Altman J; Beck W; Vrana KE *p*-Ethynylphenylalanine: A Potent Inhibitor of Tryptophan Hydroxylase. J. Neurochem 2008, 74, 2067–2073.

(53). Kypr J; Kejnovská I; Renčiuk D; Vorlíčková M Circular Dichroism and Conformational Polymorphism of DNA. Nucleic Acids Res. 2009, 37, 1713–1725. [PubMed: 19190094]

(54). Guroff G Irreversible *in Vivo* Inhibition of Rat Liver Phenylalanine Hydroxylase by *p*-Chlorophenylalanine. Arch. Biochem. Biophys 1969, 134, 610–611. [PubMed: 5354778]

(55). Kilbey MM; Harris RT Behavioral, Biochemical and Maturation Effects of Early DL-para-Chlorophenylalanine Treatment. Psychopharmacologia 1971, 19, 334–346. [PubMed: 4254728]

(56). Lipton MA; Gordon R; Guroff G; Udenfriend S *p*-Chlorophenylalanine-Induced Chemical Manifestations of Phenylketonuria in Rats. Science 1967, 156, 248–250. [PubMed: 6067026]

(57). Vorhees CV; Butcher RE; Berry HK Progress in Experimental Phenylketonuria: A Critical Review. Neurosci. Biobehav. Rev 1981, 5, 177–190. [PubMed: 6453302]

(58). Koe BK; Weissman A *p*-Chlorophenylalanine: A Specific Depletor of Brain Serotonin. J. Pharmacol. Exp. Ther 1966, 154, 499–516. [PubMed: 5297133]

(59). Kent AD; Spiropulos NG; Heemstra JM General Approach for Engineering Small-Molecule-Binding DNA Split Aptamers. Anal. Chem 2013, 85, 9916–9923. [PubMed: 24033257]

(60). Yang K-A; Chun H; Zhang Y; Pecic S; Nakatsuka N; Andrews AM; Worgall TS; Stojanovic MN High-Affinity Nucleic-Acid-Based Receptors for Steroids. ACS Chem. Biol 2017, 12, 3103–3112. [PubMed: 29083858]

(61). Mocci F; Laaksonen A Insight into Nucleic Acid Counterion Interactions from Inside Molecular Dynamics Simulations is “Worth Its Salt”. Soft Matter 2012, 8, 9268–9284.

(62). Bakker E So, You Have a Great New Sensor. How Will You Validate It? ACS Sensors 2018, 3, 1431–1431. [PubMed: 30139264]

(63). Stein WH; Moore S The Free Amino Acids of Human Blood Plasma. J. Biol. Chem 1954, 211, 915–926. [PubMed: 13221597]

(64). Jervis GA; Drejza EJ Phenylketonuria: Blood Levels of Phenylpyruvic and ortho-Hydroxyphenylacetic Acids. Clin. Chim. Acta 1966, 13, 435–441. [PubMed: 5927335]

(65). Huebert ND; Schwach V; Richter G; Zreika M; Hinze C; Haegele KD The Measurement of β-Phenylethylamine in Human Plasma and Rat Brain. Anal. Biochem 1994, 221, 42–47. [PubMed: 7985801]

(66). Clancy B; Kersh B; Hyde J; Darlington RB; Anand KJS; Finlay BL Web-Based Method for Translating Neurodevelopment from Laboratory Species to Humans. Neuroinformatics 2007, 5, 79–94. [PubMed: 17426354]

(67). Workman AD; Charvet CJ; Clancy B; Darlington RB; Finlay BL Modeling Transformations of Neurodevelopmental Sequences across Mammalian Species. J. Neurosci 2013, 33, 7368–7383. [PubMed: 23616543]

(68). Larsen DD; Callaway EM Development of Layer-Specific Axonal Arborizations in Mouse Primary Somatosensory Cortex. J. Comp. Neurol 2006, 494, 398–414. [PubMed: 16320250]

(69). Lovenberg W; Jequier E; Sjoerdsma A Tryptophan Hydroxylation: Measurement in Pineal Gland, Brainstem, and Carcinoid Tumor. Science 1967, 155, 217–219. [PubMed: 6015530]

(70). Somerville AR; Whittle BA The Interrelation of Hypothermia and Depletion of Noradrenaline, Dopamine and 5-Hydroxytryptamine from Brain by Reserpine, p-Chlorophenylalanine and α-Methylmetatyrosine. Br. J. Pharmacol. Chemother 1967, 31, 120–131. [PubMed: 6055247]

(71). Zimmer L; Luxen A; Giacomelli F; Pujol J-F Short- and Long-Term Effects of *p*-Ethynylphenylalanine on Brain Serotonin Levels. Neurochem. Res 2002, 27, 269–275. [PubMed: 11958527]

(72). Hsia DYY; Driscoll KW; Troll W; Eugene Knox W Detection by Phenylalanine Tolerance Tests of Heterozygous Carriers of Phenylketonuria. Nature 1956, 178, 1239–1240. [PubMed: 13387681]

(73). Chen H In Atlas of Genetic Diagnosis and Counseling; Chen H, Ed.; Springer New York: New York, NY, 2016.

(74). Stojanovic MN; de Prada P; Landry DW Aptamer-Based Folding Fluorescent Sensor for Cocaine. J. Am. Chem. Soc 2001, 123, 4928–4931. [PubMed: 11457319]

(75). Idili A; Gerson J; Parolo C; Kippin T; Plaxco KW An Electrochemical Aptamer-Based Sensor for the Rapid and Convenient Measurement of L-Tryptophan. Anal. Bioanal. Chem 2019, 411, 4629–4635. [PubMed: 30796485]

(76). Ricci F; Vallée-Bélisle A; Simon AJ; Porchetta A; Plaxco KW Using Nature's "Tricks" to Rationally Tune the Binding Properties of Biomolecular Receptors. Acc. Chem. Res 2016, 49, 1884–1892. [PubMed: 27564548]

(77). Zhao C; Xu X; Bae S-H; Yang Q; Liu W; Belling JN; Cheung KM; Rim YS; Yang Y; Andrews AM; Weiss PS Large-Area, Ultrathin Metal-Oxide Semiconductor Nanoribbon Arrays Fabricated by Chemical Lift-Off Lithography. Nano Lett. 2018, 18, 5590–5595. [PubMed: 30060654]

(78). National Institutes of Health Consensus Development Conference Statement: Phenylketonuria: Screening and Management, October 16–18, 2000 Pediatrics 2001, 108, 972–982. [PubMed: 11581453]

(79). Kand'ár R; Žáková P Determination of Phenylalanine and Tyrosine in Plasma and Dried Blood Samples Using HPLC with Fluorescence Detection. J. Chromatogr. B 2009, 877, 3926–3929.

(80). Haghighi F; Talebpour Z; Amini V; Ahmadzadeh A; Farhadpour M A Fast High Performance Liquid Chromatographic (HPLC) Analysis of Amino Acid Phenylketonuria Disorder in Dried Blood Spots and Serum Samples, Employing C18 Monolithic Silica Columns and Photo Diode Array Detection. Anal. Methods 2015, 7, 7560–7567.

(81). Casey CN; Campbell SE; Gibson UJ Phenylalanine Detection Using Matrix Assisted Pulsed Laser Evaporation of Molecularly Imprinted Amphiphilic Block Copolymer Films. Biosens. Bioelectron 2010, 26, 703–709. [PubMed: 20655191]

(82). Zhang K; Yan H-T; Zhou T Spectrofluorimetric Determination of Phenylalanine Based on Fluorescence Enhancement of Europium Ion Immobilized With Sol–Gel Method. Spectrochim. Acta, Part A 2011, 83, 155–160.

(83). Arakawa T; Koshida T; Gessei T; Miyajima K; Takahashi D; Kudo H; Yano K; Mitsubayashi K Biosensor for L-Phenylalanine Based on the Optical Detection of NADH Using a UV Light Emitting Diode. Microchim. Acta 2011, 173, 199–205.

(84). Girotti S; Ferri E; Ghini S; Budini R; Carrea G; Bovara R; Piazzi S; Merighi R; Roda A Bioluminescent Flow Sensor for L-Phenylalanine Determination in Serum. Talanta 1993, 40, 425–430. [PubMed: 18965647]

(85). Thiessen G; Robinson R; De Los Reyes K; Monnat RJ; Fu E Conversion of a Laboratory-Based Test for Phenylalanine Detection to a Simple Paper-Based Format and Implications for PKU Screening in Low-Resource Settings. Analyst 2015, 140, 609–615. [PubMed: 25427275]

(86). Robinson R; Wong L; Monnat JR; Fu E Development of a Whole Blood Paper-Based Device for Phenylalanine Detection in the Context of PKU Therapy Monitoring. Micromachines 2016, 7, 28.

(87). Gouda MD; Kumar MA; Thakur MS; Karanth NG Enhancement of Operational Stability of an Enzyme Biosensor for Glucose and Sucrose Using Protein Based Stabilizing Agents. Biosens. Bioelectron 2002, 17, 503–507. [PubMed: 11959471]

(88). Naghib SM; Rabiee M; Omidinia E Electrochemical Biosensor for L-Phenylalanine Based on a Gold Electrode Modified with Graphene Oxide Nanosheets and Chitosan. Int. J. Electrochem. Sci 2014, 9, 2301–2315.

(89). Zaidi SA Facile and Efficient Electrochemical Enantiomer Recognition of Phenylalanine Using β-Cyclodextrin Immobilized on Reduced Graphene Oxide. Biosens. Bioelectron 2017, 94, 714–718. [PubMed: 28395254]

(90). Reina G; González-Domínguez JM; Criado A; Vázquez E; Bianco A; Prato M Promises, Facts and Challenges for Graphene in Biomedical Applications. Chem. Soc. Rev 2017, 46, 4400–4416. [PubMed: 28722038]

(91). Omidinia E; Shadjou N; Hasanzadeh M Aptamer-Based Biosensor for Detection of Phenylalanine at Physiological pH. Appl. Biochem. Biotechnol 2014, 172, 2070–2080. [PubMed: 24326680]

(92). Hasanzadeh M; Zargami A; Baghban HN; Mokhtarzadeh A; Shadjou N; Mahboob S Aptamer-based Assay for Monitoring Genetic Disorder Phenylketonuria (PKU). Int. J. Biol. Macromol 2018, 116, 735–743. [PubMed: 29777816]

(93). Illangasekare M; Yarus M Phenylalanine-Binding RNAs and Genetic Code Evolution. J. Mol. Evol 2002, 54, 298–311. [PubMed: 11847556]

(94). Zhu Q; Shibata T; Kabashima T; Kai M Inhibition of HIV-1 Protease Expression in T Cells Owing to DNA Aptamer-Mediated Specific Delivery of siRNA. Eur. J. Med. Chem 2012, 56, 396–399. [PubMed: 22907035]

(95). Shedlovsky A; McDonald JD; Symula D; Dove WF Mouse Models of Human Phenylketonuria. Genetics 1993, 134, 1205–1210. [PubMed: 8375656]

(96). Fraser LA; Cheung Y-W; Kinghorn AB; Guo W; Shiu SC-C; Jinata C; Liu M; Bhuyan S; Nan L; Shum HC; Tanner JA Microfluidic Technology for Nucleic Acid Aptamer Evolution and Application. Advanced Biosystems 2019, 3, 1900012.

(97). Liao W-S; Cheunkar S; Cao HH; Bednar HR; Weiss PS; Andrews AM Subtractive Patterning *via* Chemical Lift-Off Lithography. Science 2012, 337, 1517–1521. [PubMed: 22997333]

(98). Xu X; Yang Q; Cheung KM; Zhao C; Wattanatorn N; Belling JN; Abendroth JM; Slaughter LS; Mirkin CA; Andrews AM; Weiss PS Polymer-Pen Chemical Lift-Off Lithography. Nano Lett. 2017, 17, 3302–3311. [PubMed: 28409640]

(99). Slaughter LS; Cheung KM; Kaappa S; Cao HH; Yang Q; Young TD; Serino AC; Malola S; Olson JM; Link S; Häkkinen H; Andrews AM; Weiss PS Patterning of Supported Gold Monolayers via Chemical Lift-Off Lithography. Beilstein J. Nanotechnol 2017, 8, 2648–2661. [PubMed: 29259879]

(100). Rim YS; Bae S-H; Chen H; Yang JL; Kim J; Andrews AM; Weiss PS; Yang Y; Tseng H-R Printable Ultrathin Metal Oxide Semiconductor-Based Conformal Biosensors. ACS Nano 2015, 9, 12174–12181. [PubMed: 26498319]

(101). Price CP; Kricka LJ Improving Healthcare Accessibility Through Point-of-Care Technologies. Clin. Chem 2007, 53, 1665–1675. [PubMed: 17660275]

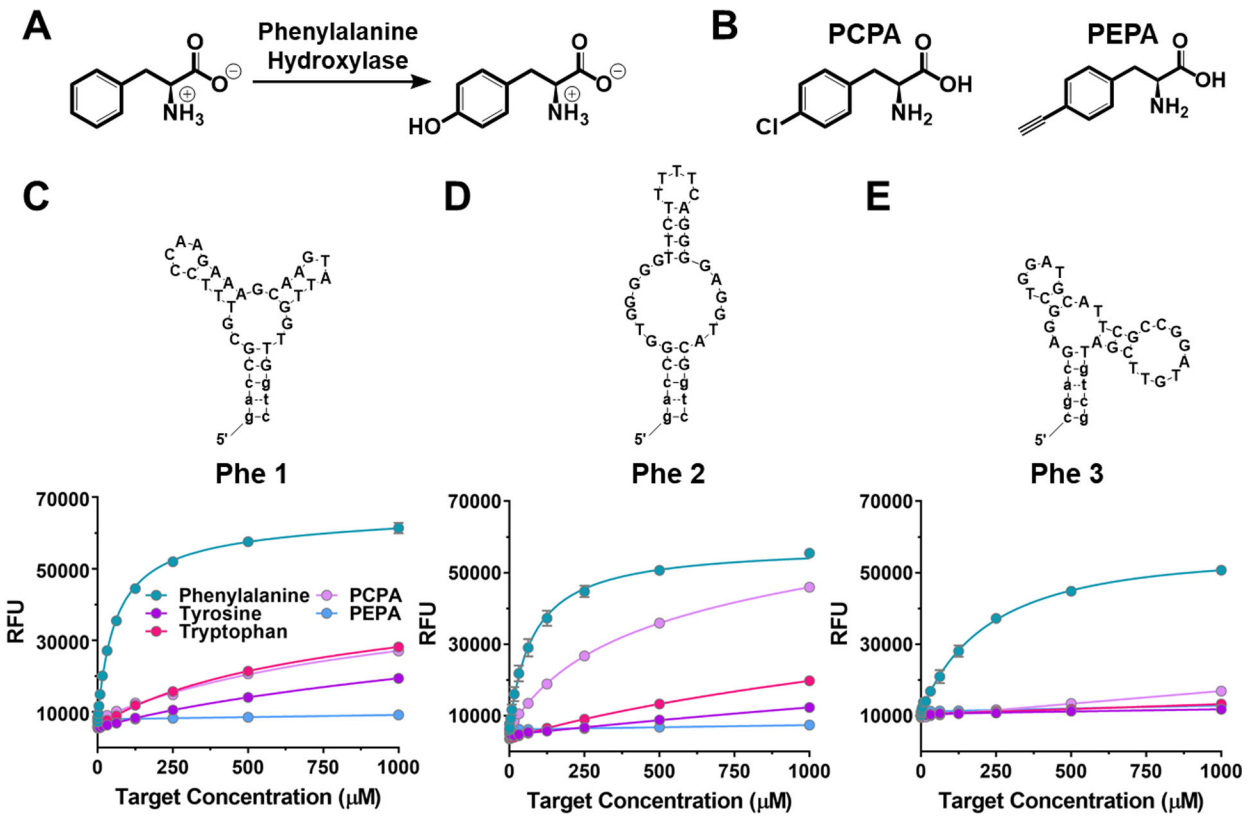

Figure 1. Aptamers for phenylalanine.

(A) In humans and mice, phenylalanine is *para*-hydroxylated to form tyrosine by the liver enzyme phenylalanine hydroxylase (PAH). The genetic disorder phenylketonuria is caused by mutations in the PAH gene, which result in high blood and brain levels of phenylalanine. **(B)** Phenylalanine analogs *para*-chlorophenylalanine (PCPA) and *para*-ethynylphenylalanine (PEPA). **(C-E)** Three phenylalanine-specific aptamer sequences (Phe 1, Phe 2, and Phe 3) were isolated for sensor development. All three aptamers showed concentration-dependent responses towards phenylalanine determined *via* competitive fluorescence assays. Responses were measured for other aromatic amino acids (tyrosine and tryptophan) and the phenylalanine analogs (PCPA and PEPA). Fluorescence concentration curves enabled determination of solution dissociation constants (K_d) for Phe 1 (10 μM), Phe 2 (7 μM), and Phe 3 (16 μM). Here, N=6 for each phenylalanine concentration; N=3 for each nonspecific target concentration. Standard errors of the means for each datum were too small to be displayed in some cases; RFU is relative fluorescence units.

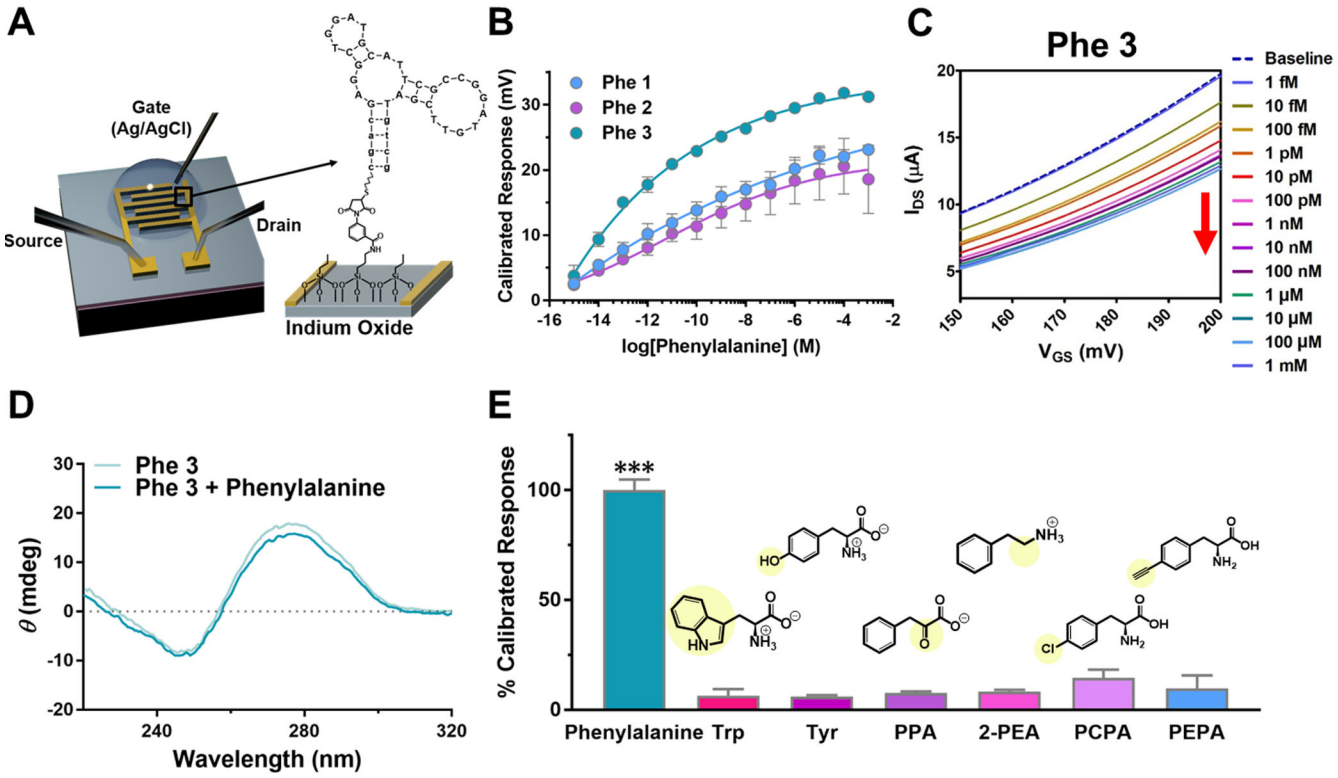

Figure 2. Detection of phenylalanine *via* aptamer-field-effect transistor sensors.

(A) Schematic of the FET platform and surface chemistry. Here, FETs were composed of 4-nm thin-film In_2O_3 as the channel material, with a 10-nm Ti adhesion layer and a 30-nm top Au layer patterned as interdigitated electrodes over the semiconductor layer. Sensing was performed by applying a source-drain bias voltage, sweeping the gate voltage with respect to a Ag/AgCl reference electrode in a solution-gated configuration, and measuring changes in source-drain currents. Thiolated aptamers were tethered to semiconductor surfaces using *m*-maleimidobenzoyl-*N*-hydroxysuccinimide ester to crosslink thiol groups to amine-terminated silanes, co-self-assembled with methyl-terminated silanes, which served as spacer molecules to optimize aptamer surface densities for target recognition. **(B)** Each of three phenylalanine aptamers attached to FETs (Phe 1, Phe 2, Phe 3) produced concentration-dependent responses in 1× Ringer's solution. **(C)** Representative transfer (I_{DS}-V_{GS}) curves for Phe 3 aptamer-FETs upon increasing phenylalanine concentrations. **(D)** Circular dichroism spectra of Phe 3 in 1× Ringer's solution before and after introduction of phenylalanine (2 µM). Spectra shown are averages of N=3 spectra each. **(E)** The Phe 3 aptamer, when incorporated into FETs, had negligible responses to nonspecific targets, including tryptophan (Trp), tyrosine (Tyr), phenylypyruvic acid (PPA), 2-phenylethylamine (2-PEA), *para*-chlorophenylalanine (PCPA), or *para*-ethynylphenylalanine (PEPA) compared to phenylalanine (all targets at 100 µM) [$F(6, 10)=76$; $P<0.001$]. Error bars, are standard errors of the means with N=3 for **B**, and N=3 for phenylalanine, PCPA, and PEPA and N=2 for Trp, Tyr, PPA, and 2-PEA in **E**. ***$P<0.001$ *vs.* all nonspecific targets.

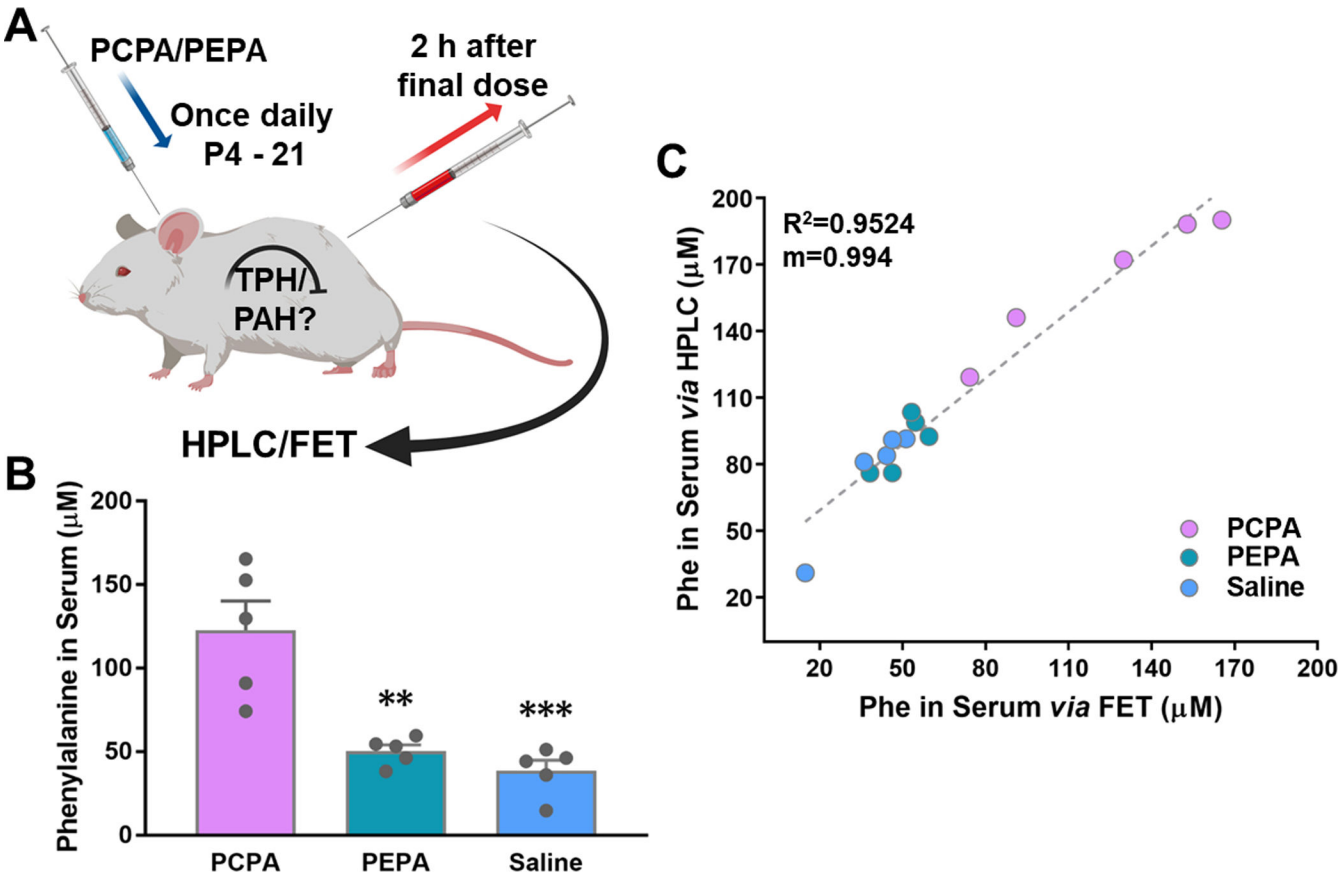

Figure 3. Aptamer-field-effect transistors (FETs) differentiate serum phenylalanine levels.

(A) Schematic illustration of the *in vivo* experimental design. Mice were treated once per day with *para*-chlorophenylalanine (PCPA) or *para*-ethynylphenylalanine (PEPA) during postnatal days (P)4–21. These phenylalanine analogs inhibit tryptophan hydroxylase (TPH). Some studies suggest that PCPA may *also* inhibit phenylalanine hydroxylase (PAH). Serum samples were collected 2 h after the final injection of each analog on P21. Phenylalanine concentrations were measured by Phe 3-aptamer-FETs and cross-correlated with high-performance liquid chromatography (HPLC) as a reference method (Figure S12). **(B)** Mice treated with PCPA had modestly elevated serum phenylalanine concentrations compared to mice treated with PEPA or saline [$F(2,12)=17.3$; $P<0.01$]. Data points depict levels from individual animals. Error bars are standard errors of the means with $N=5$ for each treatment group. $^{**}P<0.01$ *vs.* PCPA; $^{***}P<0.001$ *vs.* PCPA. **(C)** Correlation of phenylalanine concentrations measured in individual mouse serum samples *via* aptamer-FETs *vs.* HPLC with the corresponding linearity index (R^2) and regression slope (m). $P=0.762$ (Run's test), deviation from linearity is not significant.

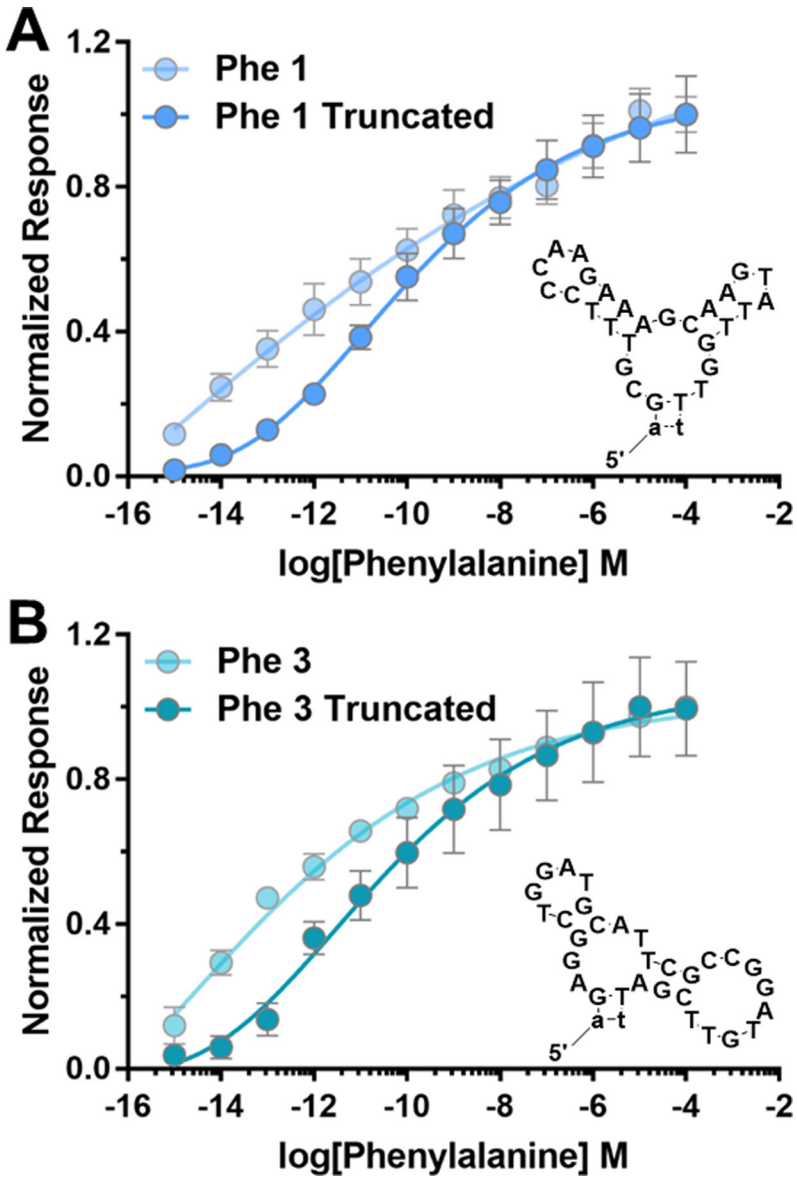

Figure 4. Tuning aptamer-field-effect transistor (FET) responses *via* aptamer stem truncation.
(A-B) Aptamer-FET sensing of phenylalanine with truncated versions of Phe 1 and Phe 3 aptamers, respectively (truncated sequences are shown in the corresponding insets). Normalized response data for phenylalanine sensing on FETs using unmodified Phe 1 and Phe 3 sequences are presented for comparison and are reproduced from Figure 2B. Error bars are standard errors of the means with N=3 for all data.